



About the return period of a catastrophe

Mathias Raschke¹

¹Freelancer/independent researcher, Stolze-Schrey-Str.1, 65195 Wiesbaden, Germany

Correspondence to: Mathias Raschke (mathiasraschke@t-online.de.com)

5 **Abstract.** To understand catastrophes like earthquakes stochastically, their return period (RP) should be quantified for the
concerned region. Measures such as event magnitudes or indexes are less helpful for this purpose. We derive the combined
return period (CRP) from the pseudo-polar coordinates of extreme value theory. The CRP is the (weighted) mean of local RPs
and is again an RP; other metrics do not provide such testable reproducibility. We demonstrate CRP's opportunities on
extratropical cyclones (winter storms) over Germany, including validation and bias correction of local RP estimates.
10 Furthermore, we introduce new estimation methods for the RP of an event loss (risk curve) via CRP-scaling of historical storm
fields. For high RP, the resulting event losses of the German insurance market are higher in the case of max-stable dependence.
The latter means the same dependence level between local maxima of a year as of a decade. However, spatial dependence is
not stable but decreases by increasing period. Such control of spatial dependence is not realized by previous risk models from
science and industry. Our loss estimates for RP of 200 years are also significantly smaller than those of European regulation's
15 standard model.

1 Introduction

When a natural catastrophe (NatCat) such as a large windstorm or an earthquake has occurred, the question arises, how often
such random events appear, i.e., what is the corresponding return period (RP, also called recurrence interval)? Before
discussing this issue, we underline that the extension of river floods or windstorms in time and space depend on the scientific
20 and socio-economic event definition. These are not our topic even though they influence our research object – the RP.
The RP of an event magnitude or index is frequently used as a stochastic measure of a catastrophe. For example, there are
different magnitudes scales for earthquakes (Bormann and Saul, 2009). Unfortunately, corresponding RPs for the source region
may not correspond well with the catastrophic consequences since the hypocentre position also determines destructiveness.
For floods, regional or global magnitude scales are not in use (Guse et al., 2020). For hurricanes, the Saffir–Simpson scale
25 (National Hurricane Centre, 2020) is a magnitude measure; but the random storm track also influences the destruction's extent
of the destruction. Extratropical cyclones hitting Europe, called winter storms, are measured by a storm severity index (SSI;
Roberts et al., 2014) or extreme wind index (EWI; Della-Marta et al., 2009). Their different definitions result in quite different
RP for the same events. Also, their statistical models include assumptions and pitfalls. In rare scientific publications about risk
modeling for the insurance industry, such as by Mitechell-Wallace et al. (2017), better and universal approaches for the RP
30 are not offered. In sum, previous approaches are not very fruitful. Nevertheless, RP is needed to understand and manage NatCat



risk by decision-makers in administration, policy, and industry and research the consequences of climate change (Della-Marta et al. 2010, Schwierz et al. 2010). In the end, the RP of losses and damage (the risk curve) is needed.

For these reasons, at first, we derive from extreme value theory a flexible and reproductive stochastic measure for a NatCat in a defined region – the combined return period (CRP). Then, we explain implications and opportunities in section 2. These are
35 testability, scalability, and a variant of Raschke’s (2013) area function. We apply the concepts to extratropical cyclones (winter storms) in Germany, estimate the CRP for historical events of last decades, and test the CRP concept. Since the CRP is spatial related, we also examine spatial dependence between local hazards. Furthermore, we use the derived scaling opportunity of historical event fields to estimate a risk curve for the aggregate of insured losses per event in Germany in consideration of loss data. In section 3, we explain statistical details of the analysis of German winter storms regarding local hazard, vulnerability,
40 and uncertainties. Subsequently, we present stochastic interpretations and numerical details of the risk estimate. Finally, in section 5, we summarize and discuss our results with a focus on previous analysis of risk and spatial dependence.

2 Theory and Application of CRP

2.1 Derivation of CRP

Stochastic deals with more than only random variables. A Poisson point process or briefly Poisson process (Coles, 2001;
45 Beirlant et al., 2004; Falk et al. 2011) is also a random element with random point events at the line of real numbers. A NatCat event is measured by its local intensity (e.g., river discharge or wind gust peak) at a geographical site. This local intensity occurs (approximately) as point event of a Poisson process with points X ; the number of independent events with $X \geq x$ during a defined unit period (e.g., a season or a year) is a random integer number K that follows a Poisson distribution (Coles, 2001; Beirlant et al., 2004; Falk et al. 2011) with an expectation (expected value) $E[...]$ - the exceedance frequency (EF) function
50 (with indicator function I)

$$\Lambda(x) = E[K], K = \sum_{i=1}^{\infty} I(X_i > x). \quad (1)$$

It is a bijective function. The reciprocal of expected local EF is the local RP

$$T(x) = 1/\Lambda(x). \quad (2)$$

As X is a point event it’s RP T is also a point event and the EF function of T is

$$55 \Lambda(x) = 1/x. \quad (3)$$

It might be called the RP process. In the Supplementary (Figure 1), the EF function is depicted beside realizations, one of a single process and a second of two associated processes. In extreme value theory and statistics (Coles, 2001; Beirlant et al., 2004; Falk et al. 2011), the density of point events T at the line of positive real numbers is expressed by the Poisson process's intensity, being the negative first derivative of (3).

60 Two-point processes can be associated. According to de Haan (1984), Coles (2001) and Falk et al. (2011), two max-stable linked point processes with point events T_1 and T_2 are represented by pseudo polar coordinates with radius R and angle V

$$R = T_1 + T_2, V = \frac{T_1}{T_1 + T_2}, \text{ corresponding } T_1 = RV, T_2 = R(1 - V) = T_1 \frac{1-V}{V}. \quad (4)$$

As we describe in the Supplementary, the expectation of the random element $(1 - V)/V$ is 1 and for the conditional expectation of unknown RP T_2 with known T_1 applies (association is provided)

$$65 \quad E[T_2|T_1] = T_1. \quad (5)$$

The interest in extreme value theory and statistics (Coles, 2001; Beirlant et al., 2004; Falk et al. 2011) is focused on the distribution function of pseudo angle V with cumulative distribution function (CDF) $H(x)$. It determines the dependence structure, called copula (Marie and Kotz, 2001), of the block maxima of the processes - here local maxima of all point events T (or X) during k considered unit periods (e.g., half years, a season, years, or decades). The univariate CDF of maximum
 70 occurred RP of a k unit periods considers $\Lambda(x)$ of (1) and also of (3)

$$G_k(x) = \exp(-k\Lambda(x)) = \exp(-k/x). \quad (6)$$

If the copula of a bivariate distribution $G_k(x_1, x_2)$ of two local maxima is max-stable, the dependence between annual maxima is the same as between century maxima. It is also called extreme value copula (Marie and Kotz, 2001). The independence gives this max-stability of the dependence structure between pseudo angle V and pseudo radius R in (4) (Coles, 2001). The
 75 occurrence of the pseudo radius is once again a point process with EF $\Lambda(x) = 2/x$ - the double of (3). This means the average of two RP T_1 and T_2 results in a combined return period (CRP) T_c with EF function (3). This applies for the max-stable case between the limits - full dependence ($T_1 = T_2$) and no dependence ($T_1 = 0$ if $T_2 > 0$ and vice versa, $T_i = 0$ represents the lack of a local event). These are also the limits of non-max-stable dependence structures. Therefore, CRP should also apply for non-max-stable dependence, which can be validated heuristically as shown in the Supplementary. The critical result is that the
 80 average of two RPs is again an RP with EF (3). Such reproductivity does not apply to a metric of the EF or the logarithm of RP. RP has probably been averaged in NatCat studies before, but it was not known that this average remains an RP.

A weighting w in the averaging is also possible because of the commutative property of numbers

$$T_c = \frac{\sum_{i=1}^n T_i w_i}{\sum_{j=1}^n w_j}. \quad (7)$$

The continuous version via a defined region in a geographical space with coordinates z is

$$85 \quad T_c = \frac{\int_{region} T(z)w(z)dz}{\int_{region} w(z)dz}. \quad (8)$$

For weight $w(z) = 1$, the integral in the denominator is the area of the region.

2.2 Opportunities and implications

A sample of CRPs can be tested by a comparison of its EF function (3) and their empirical variant. Therein the empirical EF of the largest CRP in the sample is the reciprocal of observation period. The 2nd largest CRP is hence associated to twice the
 90 EF of the largest CRP and so on. However, not all small events are recorded; the sample is thinned and incomplete in this



range. This is less important if only the distribution (6) of maximum CRPs are tested. There are a number goodness-of-fit testes (Stephens, 1986) for this situation with a known distribution model.

Besides that, the CRP offers the opportunity of stochastic scaling. The CRP T_c and all local RPs T_i in (7) or $T(z)$ in (8), and by this, the pseudo radius R in (4) are scaled via a factor S . The pseudo angle V stays the same.

$$95 \quad T_{cS} = T_c S, \quad T_s(z) = T(z) S, \quad T_{s,j} = T_j S, \quad R_s = R S, \quad V_s = V. \quad (9)$$

The corresponding event field of local intensities (e.g., maximum wind gust speed) can be computed for the scaled RPs via the inverse of the EF function (1) of local intensity. If the association between the local point processes is max-stable, the value of $H(V)$ is not changed, and nothing is changed in the sampling regarding dependence. This matches the scaling in Schlatter's (2002) two theorems about max-stable random fields (by Schlatter's random elements). Such simple scalability does not
100 apply if we lack max-stability in the spatial dependence; an extensive scaling without special considerations would be critical because of uncontrolled consequences.

A further opportunity is to present all local RPs of an event in a defined region via Raschke's (2013) cumulative area function, which is normalized here to provide comparability.

$$A(x) = \frac{\int_z w(z) I(T(z)) dz}{\int_z w(z) dz}, \quad I(T(z)) = 1 \text{ if } T(z) \geq x, \text{ otherwise } I(T(z)) = 0. \quad (10)$$

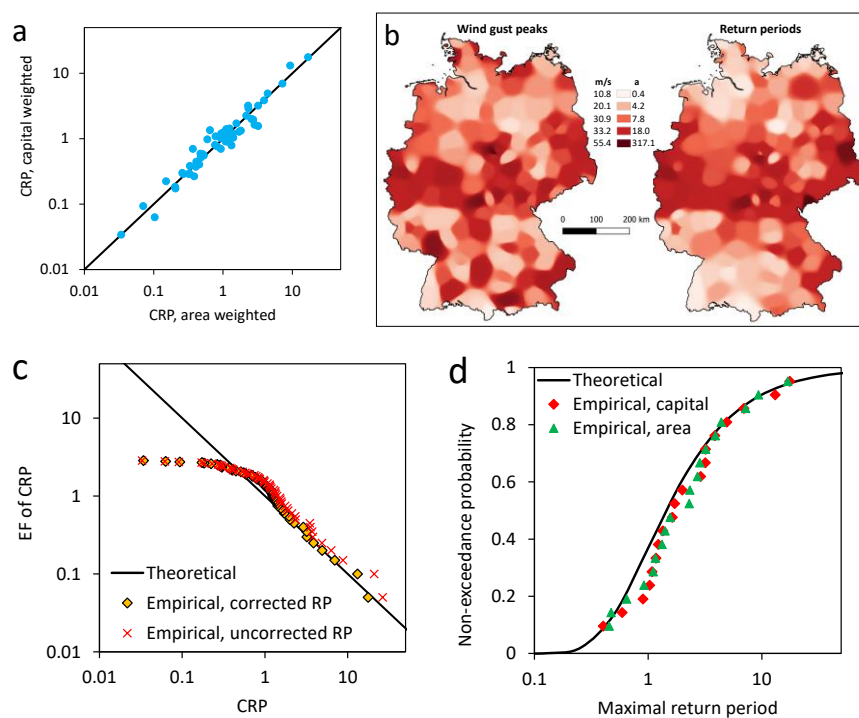
105 Jung and Schindler (2019) have recently published a similar cumulative presentation for local wind speed maxima of storm events. The function $A(x)$ is like the survival function of a (conditional) random variable, here the local RPs of the event. The CRP T_c represents the expectation (or its estimate). It can also be derived from the moments of random variables that the coefficient of variation (CV; Upton and Cook, 2008) for (10) is not be concerned about scaling (9) for max-stable situations. This implies that the CV is independent of CRP in the case of max stability. This underlines that the CRP and area function
110 corresponds with maxima's spatial dependence in the sense of max-stable random fields (Schlather, 2002).

2.3 Analysis of German Winter Storms

To demonstrate the application of CRP, we analyze 57 winter storms (also called winter windstorms) over Germany over 20 years, from autumn 1999 to spring 2019. Wind station data have been provided by the German meteorological service (DWD, 2020). Different completeness criteria were considered for station selection, and different references (Klawns and Ulbrich, 2003; Gesamtverband Deutscher Versicherer, 2019; Deutsche Rück, 2020) have been considered for selecting the time window
115 per event. The lists are presented in the Supplementary (Excel file). The one and a half-power of wind speed maximum are analyzed as local peril intensity. The reason is explained in Section 3.1 and the appropriateness of the Gumbel distribution for the block maxima of local event intensities and corresponding computation of RP per event with bias correction. To increase the accuracy of estimates by higher sample size, we analyze the maxima of half-seasons per station. The computed CRPs are
120 also listed in the Supplementary. We considered simplified area weights and the grid's capital weights from Global Assessment Report (GAR; UNISDR, 2015), assigned to the wind station by shortest distance. The first variant considers the storm as a



pure phenomenon in the geographical space; the second is more focused on consequences. The significant storm Kyrill (2007) has CRPs of 16.97 ± 1.75 and 17.64 ± 1.81 years (area and capital). Both are around in the middle of the estimated range 15 to 20 years by Donat et al. (2011). CRPs are compared in Figure 1 a for a one-year unit period (equal to one season). For example, the simply interpolated event fields (one is the wind field) for Kyrill are shown in Figure 1 b. In Figure 1 d and e, the results are validated. The empirical EF matches well with the theoretical one for $T_c \geq 1.65$. Small CRPs are affected by the incompleteness of records. In the medium range, the differences between the model and empiricism are not statistically significant (for $T_c \geq 1$ probability of 7.8% for the 27 exceedances or more for 20 years). The bias correction of local RP affects higher CRPs (Figure 1 c). In Figure 1 d, the maximum CRP of a season follows the CDF (6) very well. The Kolmogorov-Smirnov (KS) test (Stephens, 1986) for fully specified distribution accepts the model for the extreme high significance level of 25% (the pure KS statistic is 0.1422, sample size $n = 20$). Usually, level 5% is used; however. The KS test should not be affected seriously by the absence of one (probably the smallest) maximum due to an incomplete event list.



135 **Figure 1: Results of the analysis: a) comparison of area and capital weighted CRPs, b) Storm Kyrill, 2007, inverse distance weighting (by software Qgis with distance parameter 6) for local wind peaks as reproduction of the wind field and field of local RP (same colour - same percentile), c) comparison of theoretical and observed EF of capital weighted CRPs with influence of correction, d) test of distribution of maxima of CRP with capital weighting of a seasons (equivalent with annual maxima).**

As aforementioned, the CRP corresponds with the dependence between local RPs. Therefore, the characteristic of spatial
 140 dependence between block maxima is also analyzed. The plot of the estimates of dependence measure Kendall's τ (Upton and Cook, 2008) is depicted in Figure 2 b. It decreases by increasing distance. The scatter range of the half seasons is smaller than for two seasons due to different sample sizes. In Figure 2 c, we also compare Germany with results for Switzerland (Raschke



et al., 2011). For the latter, the spatial dependence is smaller, probably because of the alpine topography. The sample mean of Kendall's τ decreases by value 0.05 with increasing block size (half-season versus two seasons). This is statistically significant; the normally distributed confidence range of estimated expectation of the differences indicates probability 0.002 for values ≤ 0 . Max-stability is unlikely. The characteristics of spatial dependence also influence the area functions in Figure 2 c. The hypothetical case of fully spatial dependence is shown as a benchmark (CRP 100 years) and has no scattering with a CV of 0. The scaling opportunity is demonstrated by the storm Kyrill of 2007 with $T_{CS} = 100$ years. The differences between area functions of the area and capital weightings depend on the concrete storm. The CV should be independent of RP in case of max-stable dependence. This does not apply according to Figure 2 d; it increases by increasing CRP in the regression model for capital weighted CRP. The p value is 0.002 for an exponent ≤ 0 ; this confirms the non-max-stable behavior of Kendall's τ . The estimates of the exponent differ insignificantly (area versus capital weighting). Details of our more complicated proxy for non-max-stable scaling are presented in Supplementary. In Figure 2e, the relation between scaled CRP and CV of the proxy is shown. The regression function of Figure 2 d is reproduced.

155

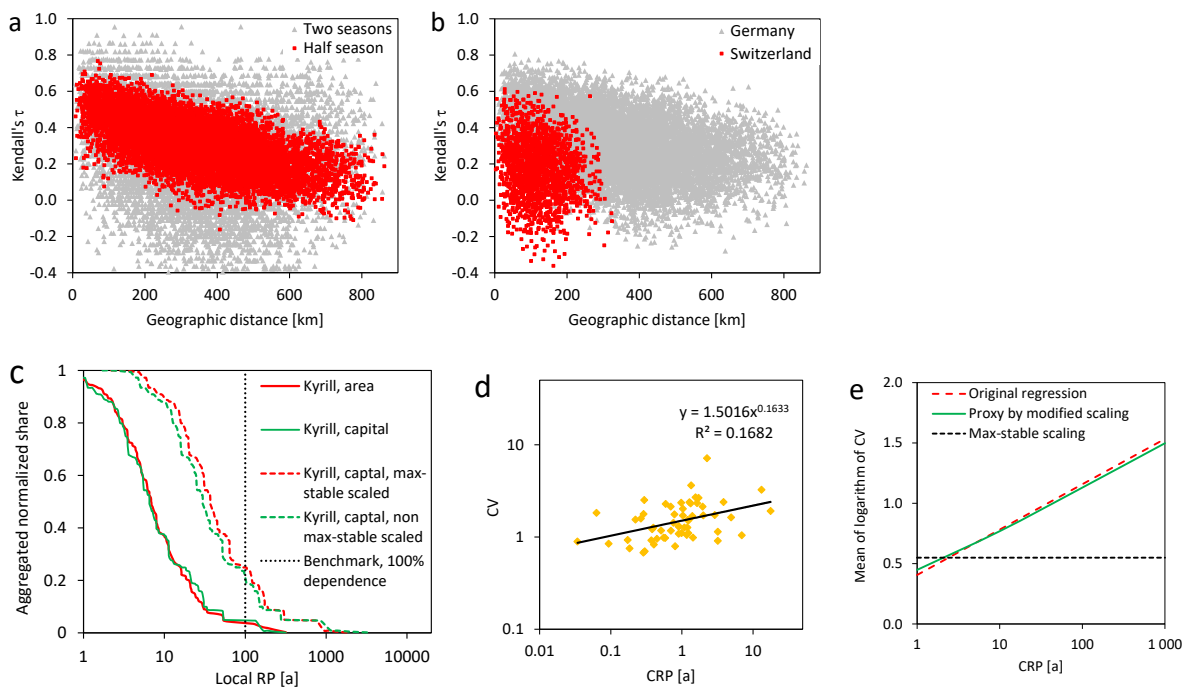


Figure 2: Spatial characteristics: a) estimated Kendall's τ versus distance for different block sizes, Germany, b) estimated Kendall's τ versus distance for a season for Germany and Switzerland (Raschke et al., 2011). c) normalized area functions, and d) CV of local RP versus CRP (capital weighted), and e) approximation of this relation by modified, non max-stable scaling.

160 2.4 Risk estimates by averaging

The interest of NatCat risk analysis is in the risk curve, i.e., the relation between an event loss L_E and its RP T_E . It is a bijective function $L_E(T_E)$ with its inverse variant $T_E(L_E)$ and can be estimated by relation (5) and our concept of scaled CRP. The latter implies a (modelled) event loss L_E for the scaled field of local RP (9) and corresponding local intensities (catchword local



hazard curve). The local intensity, vulnerability and exposure value determine the local (expected) loss. Its aggregation over
165 the geographical space determines the event losses L_E with RP T_{CS} . The stochastic link between T_{CS} and T_E is (5), and the risk
curve can be estimated by variants of averaged metrics of n scaled historical wind fields respectively corresponding wind
records

$$\hat{T}_E(L_E) = \frac{1}{n} \sum_{i=1}^n T_{CS,i}(L_E), \hat{\Lambda}_E(L_E) = \frac{1}{n} \sum_{i=1}^n 1/T_{CS,i}(L_E), \hat{L}_E(T_E) = \frac{1}{n} \sum_{i=1}^n L_{E,i}(T_{CS} = T_E). \quad (11)$$

Further details of the concept are explained and illustrated in *Section 4*.

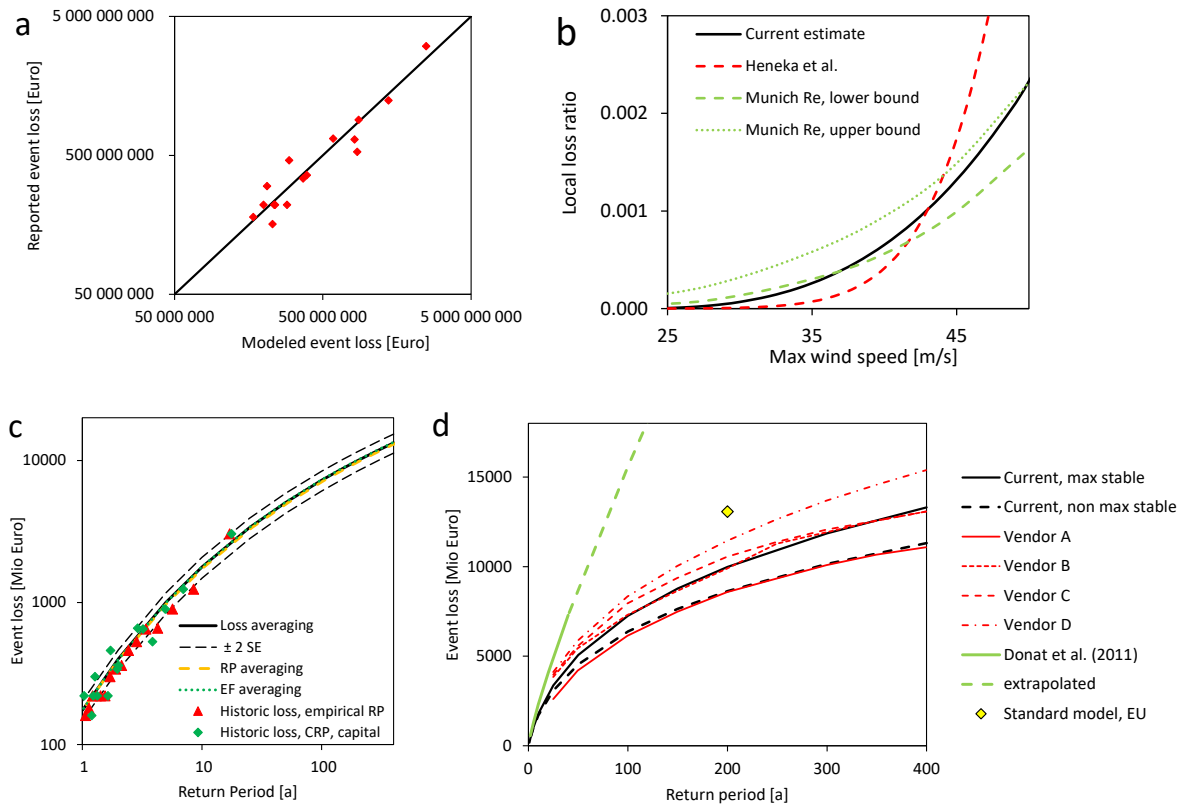
170 Our demonstration object remains Germany, and we estimate its risk curve for insured winter storm losses. The local losses
are simply the product of local exposure value and loss ratio L_R . This is determined by local maximum wind speed per event
via the (local) vulnerability function (loss or damage function). Our loss function follows the approach of Klawns and Ulbrich
(2003) and is fitted by the data of the General Association of German Insurer (GDV, 2019) for 16 historical events from 2002
to 2018 (Figure 3 a). These loss data are already inflated/scaled to the German insurance market 2018. An exemplary variant
175 of our vulnerability functions is compared to previous models in Figure 3 b; different geographical resolutions might explain
the differences. The processed model of the geographical distribution of exposed values is the same as for capital weighting
in the previous section. The assumed total sum insured (TSI) is 15.23 Trillion euros and based on the assumptions of Waisman
(2015). His TSI for Germany is scaled/inflated from 2015 to 2018 by factor 1.12 under consideration of increasing construction
prices (Statistisches Bundesamt, 2020) and building stock (GDV, 2019).

180 The three risk curves, that have been estimated by (9) with wind fields scaled by capital weighted CRP are shown in Figure 3
c. Also, reported losses of historical events⁰ and their empirical RP (observation period of 17 years) and the estimated CRP
are plotted. The differences between the risk curves are minor. The standard error (SE) of estimates by loss averaging (also
called RP scaling) is more minor than 8.5% of the estimated event loss for RP $T_E \leq 400$ years. The range of two SE is not a
confidence range for empirical RP. Its uncertainty is higher and explains the higher differences to the risk curves.

185 Since German winter storms do not imply max-stable dependence, we also estimate the risk by non-max-stable scaling. The
result is depicted in Figure 3 d and shows lower event losses for high RP than in the max-stable case. We also compare our
risk curves with these vendor models, which have been presented by Waisman (2015). However, the exposure assumptions
are not the same (exposure year, market share, split between residential, commercial, and industry). To provide comparability,
the vendor estimates are scaled by factor 1.34. This is the average of the ratios between reported and modeled loss for storm
190 Kyrill. We also consider the risk estimate by Donat et al. (2011) and the standard model of European Union (EU) regulations
(European Commission, 2014), also known as Solvency II requirements. It considers the exposure per CRESTA zone
(www.cresta.org). For the standard model, we split our assumed TSI to the Cresta zones by the GAR data. The same TSI is
used to scale Donat's et al. (2011) estimated RP for event loss ratios (NCEP variant in Figure 7); our extrapolation complies
with their distribution assumption. We highlight that we cannot fully ensure comparability to the previous risk estimates.



195



200

Figure 3: Estimates for insured losses from winter storms in Germany: a) comparison of event losses, b) vulnerability functions (current estimate with average of local parameters, previous estimates by Heneka and Ruck (2008) and Munich Re (2002) for residential buildings in Germany), c) current risk curves and observations, d) influence of asymptotic behavior of spatial dependence and comparison to (scaled) previous estimates (Donat et al., 2011; Waisman, 2015) and methods (European commission, 2014).

3 Secondary Methods in the Analysis of German Winter Storms

3.1 Modeling of local hazard

205

The local hazard curve for the EF of local event intensity must be estimated to compute the local RP by event and station for our example – winter storm over Germany. For this purpose, the relation between local event frequency and CDF of corresponding block maxima is used according to equation (3) and (6). We model the CDF of local block maxima of intensity by the Gumbel distribution. This is a special case of generalized extreme value distribution (Coles, 2001; Beirlant, et al. 2004) with extreme value index $\gamma = 0$ in the CDF

$$G(x) = \begin{cases} \exp\left(-\exp\left(\frac{x-\mu}{\sigma}\right)\right), & \text{if } \gamma = 0 \\ \exp\left(-\left(1 + \gamma \frac{x-\mu}{\sigma}\right)^{-1/\gamma}\right), & \text{if } \gamma \neq 0 \end{cases} \quad (12)$$



The scale parameter is σ , location parameter is μ . For completeness, this distribution is max-stable in a univariate sense.

210 Extreme value index γ is independent of the block size (k in equation (6)); σ is independent of the Gumbel case's block size. For a sampling of block maxima, we only consider wind speed maxima of the winter storm season that we define from September to April. A shorter definition is from October to March. The differences between the resulting block maxima are not significant. To increase the sample size, we analyze the maxima of half seasons of Autumn 1999 to Spring 2019 and have 40 observations. An entire season corresponds to one year. The distinction between block size (number of unit periods in (6))

215 were considered in the post-processing of the results. There is the opportunity that other kinds of wind perils contaminate our sample. As a specific compensation, extratropical cyclones also (albeit rarely) occur outside our sampling periods. We consider records of wind stations in Germany of DWD (2020; FX_MN003, a daily maximum of wind peaks, usually wind gust speed [m/s]) that include minimum record completeness for one of the analyzed storms of 90%, at least 90% completeness for all seasons and 55% minimum completeness per (half) season. Therefore, we only use records of 141 stations.

220 The autocorrelation between the subsequent half-season maxima has been tested, for significant level $\alpha = 5\%$ around 6% fails the test. This corresponds to the error of the first kind what is interpreted that autocorrelation is not significant. Similarly, the homogeneity test (two-sample test; Conover, 1971) rejects 5% of the pairs of samples first season half versus second season half for a significant level of 5%. Besides, we have considered the wind speed with power 1, 1.5, and 2 as the intensity in a first fit of the Gumbel distribution by the maximum likelihood method (Coles, 2011). According to these, power 1.5 offers the

225 best fit of wind gust data. Such wind measure adjustment was already suggested by Cook (1986) and Harris (1996). We do not consider the generalized extreme value distribution with index $\gamma \neq 0$ in (12) for the following reasons. It would require an extensive physical explanation if some wind stations are concerned by a finite upper bound for $\gamma < 0$ and other stations not with $\gamma \geq 0$. Besides, information criteria AIC and BIC (Lindsey, 1996) indicate that the Gumbel distribution is the better model. In addition, the share of rejected Gumbel models (one by station) of the Goodness-of-fit test (Stephens, 1986)

230 is with 6% around the defined significance level of 5%, the error of 1st kind – falsely rejected correct models. Also, when we estimate the extreme value index γ , then the standard deviation of all estimates equals the SE for estimates for actual index $\gamma = 0$ for the same sample size. All statistics indicate the Gumbel distribution. Even though we considered only stations with a high level of record completeness, not every sample is complete; some daily records are missed. This affects the sampling of block maxima and indirect likelihood (ML) estimation for their CDF. This is

235 considered in the estimates as explained in the Supplementary. An extensive Monte Carlo simulation with 100,000 repetitions for sample size $n = 40$ has been done to validate the correction's performance. We also realized that complete and incomplete samples result in a biased estimate of σ ; it is only 98% of the actual value. This ML method's bias for small sample sizes is already stated by Landwehr et al. (1979) and is corrected for our application. Furthermore, EF $\Lambda(x)$ estimates for a defined intensity level x are (more or less) unbiased. This does not apply to the estimated RP as reciprocal of EF (parameters

240 corresponds to (12))

$$\hat{T}(x) = 1/\hat{\Lambda}(x) = \exp\left(\frac{x-\hat{\mu}}{\hat{\sigma}_{cor}}\right). \quad (13)$$



245 Via the estimation results of the Monte Carlo simulation, a correction function for the local RP estimates has been derived and is presented in the Supplementary. The correction function is also applied to estimates for sample size $n = 39$ because of the small difference. The smaller sample is applied to estimate the SE of CRPs by the leave-one-out method, also called Jackknife method (Lindsey, 1996).

3.2 Modeling of vulnerability

250 To quantify the loss ratio L_R at location (wind station) j and event i , we use the approach of Klawns and Ulbrich (2003) for Germany. The difference to the origin is not significant. However, our variant has a bit higher correlation between reported and modelled loss. The event intensity x is the maximum wind gust speed. $v_{98\%}$ is the upper 2% percentile from empirical distribution of all local records. The relation is with parameter a_L

$$L_{R,i,j} = a_L \text{Max}\{0, (v_{i,j} - v_{98\%})\}^3, \quad (14)$$

Donat et al. (2011) have also used this approach but with an additional location parameter. This is discarded here since the loss ratio must be $L_R = 0$ for local wind speed $v = 0$. This is also a reason, why a simple regression analysis (Lindsey, 1996) is not applied to estimate a_L . We use

$$255 \hat{a}_L = \frac{1}{n} \sum_{i=1}^k \frac{\sum_{j=1}^n E_{j,i} \text{Max}\{0, (x - v_{98\%})\}^3}{L_{E \text{ reported}, i}}, \quad (15)$$

with k historical storms, corresponding reported event losses L_E , n wind stations, and (here modelled) local exposure value $E_{j,i}$ being assigned to the wind station. It would be the same for every station if there were wind records for every storm at each station. However, the wind records are incomplete and the assumed TSI must be split and assigned to the stations a bit differently for some storms. The normal share per station is pre-estimated by capital grid values of GAR data (normalized that sum is 1). These have been assigned to the station by the shortest distance. Our estimate for the scale parameter by (15) is 260 0.0960 ± 0.0060 . The power parameter (exponent) and upper 2% percentile in (14) are defined and influence the risk estimate. A higher power parameter would result in higher event losses for higher RP. However, an exponent larger than 3 is not likely since an exponent of 2 would be also reasonable according to building codes (European Union, 2005) with proportional relation between squared wind peaks and structural load.

265 3.3 Error estimate and accuracy

The SE of the winter storm risk estimate for Germany is only computed for the RP scaling (loss averaging). Thereby we consider three components. The uncertainty from the local hazard estimates is considered by the Jackknife method, applied synchronously by half-season for all wind stations to consider the correlation between the SE of different stations. The SE for the vulnerability function's scaling parameter in (14) and (15) is computed as the standard error of expectation being estimated



270 by the sample mean. The same applies to the loss estimated by scaled CRP of 16 historical storms. The three SE are combined under the assumption of independence as the sum of their corresponding variances (square of SE).

The shares of uncertainty components on the error variance (squared SE) of our risk estimates depend on the RP. On average of our supporting point, these are 15% for the limited sample of scaled historical events, 24% for the uncertainty of local hazard parameters, and 61% by the vulnerability model's parameter.

275 Our two weighting variants for Winter Storms over Germany correlate much better with Kendall's $\tau = 0.814$ and Spearman's $\rho = 0.946$ than the RPs of Della-Marta's⁰ et al. event measures for European windstorms. The accuracy of the current RP estimates is also slightly higher than these of Della-Marta et al. For instance, an estimated RP 15-20 years has a SE smaller than two years currently; Della-Marta et al. report RP a range of 14 years for the 95% confidence interval. This is approximately equivalent to SE of more than three years. The current precision of the German storm risk estimate with a sample of 16
280 historical storms is also higher than the estimates by Donat et al. (2011) with a sample of 30 historical storms.

3.4 RP of vendor's risk estimate

We compare our results with vendor models. These have estimated the risk curve for the maximum event loss within a year. This is a random variable, and their pseudo-RP is the reciprocal of the exceedance probability. This pseudo RP can never be smaller than 1. We transform pseudo RP to an event one by the relation between EF and CF in (6). With increasing event loss,
285 the difference between its pseudo RP and the actual one converges to 0. The concrete name of the vendors can be found in Waisman's (2015) publication. The reader should be aware that the vendors might have updated their winter storm model for Germany in the meantime.

4 Remarks on risk estimate by averaging

4.1 Details of the procedure

290 Our estimation variants are formulated by (11). For the concrete computation, elements and steps are depicted in the schemes in Figure 4 and Figure 5.



1. Determining scaled CRP by selection of RP of event loss $T_{CS} = T_E$
2. Loop A – for each historical event i
3. Scaling factor $S_i = T_{CS,i}/T_E$ according to (9)
4. Loop B – for each wind station j
5. For non-max-stable case scaling correction by $S_{j,i} = \exp(a_j \ln(S_i)^2 + b_j \ln(S_i) + c_j)$ and $S_{j,i} = S_i^{1+c_j T_{j,i}/T_{CS,i}}$
6. Scaling of local RP by $T_{S,j,i} = T_j S_i$ for max-stable case, otherwise by $T_{S,j,i} = T_j S_{j,i}$, $T_{j,i}$ –RP of historical storm i at station j
7. Inverse bias correction of scaled local RP by higher solution value for $T_{bias S,j,i}$ in $\ln(2 T_{S,j,i}) = -0.00742 \ln(2 T_{bias S,j,i})^2 + 0.97920 \ln(2 T_{bias S,j,i}) - 0.01356$ with factor 2 since half seasons are sampled and full seasons/years are modelled
8. Computing local event intensity by inverse of local hazard function $x_{j,i} = \hat{\sigma}_{cor,j} \ln(T_{bias S,j,i}) + \hat{\mu}_j$
9. Transfer of event intensity to pure wind speed $v_{j,i} = x_{j,i}^{2/3}$
10. Computing local loss ratio $L_{R,i,j} = a_L \text{Max}\{0, (v_{j,i} - v_{98\%j})\}^3$
11. Computing local loss $L_{E,i,j} = L_{R,i,j} E_{j,i}$
12. Aggregation of local loss $L_{E,i} = \sum_{j=1}^n L_{E,i,j}$ during loop B
- End of Loop B
- End of Loop A
13. Risk estimation by averaging of losses $\hat{L}_E(T_E) = \frac{1}{n} \sum_{i=1}^n L_{E,i}$

Figure 4: Computation elements and steps for RP scaling – loss averaging.

1. Determining event loss L_E
2. Loop A – for each historical event i
3. Numerical goal seek for scaling factor S_i and which result in determined event loss L_E
4. Corresponding RP $T_{CS,i} = S_i T_{CS,i}$
5. Loop B – for each wind station j
6. Scaling of local RP by $T_{S,j,i} = T_j S_i$, $T_{j,i}$ –RP of historical storm i at station j
7. Inverse bias correction of scaled local RP by higher solution value for $T_{bias S,j,i}$ in $\ln(2 T_{S,j,i}) = -0.00742 \ln(2 T_{bias S,j,i})^2 + 0.97920 \ln(2 T_{bias S,j,i}) - 0.01356$ with factor 2 since half seasons are sampled and full seasons/years are modelled
8. Computing local scaled event intensity by inverse of local hazard function $x_{j,i} = \hat{\sigma}_{cor,j} \ln(T_{bias S,j,i}) + \hat{\mu}_j$
9. Transfer of event intensity to pure wind speed $v_{j,i} = x_{j,i}^{2/3}$
10. Computing local loss ratio $L_{R,i,j} = a_L \text{Max}\{0, (v_{j,i} - v_{98\%j})\}^3$
11. Computing local loss $L_{E,i,j} = L_{R,i,j} E_{j,i}$
12. Aggregation of event loss $L_{E,i} = \sum_{j=1}^n L_{E,i,j}$ of event i during loop B
- End of Loop B
- End of numerical goal seek, if $L_{E,i}$ equals the determined values
- End of Loop A
13. Risk estimation by averaging of RP $\hat{T}_E(L_E) = \frac{1}{n} \sum_{i=1}^n T_{CS,i}$ or EF $\hat{\Lambda}_E(L_E) = \frac{1}{n} \sum_{i=1}^n 1/T_{CS,i}$

295 **Figure 5 Computation elements and steps for Loss scaling – RP or EF averaging (only for the max-stable case).**

4.2 Stochastic background and interpretation

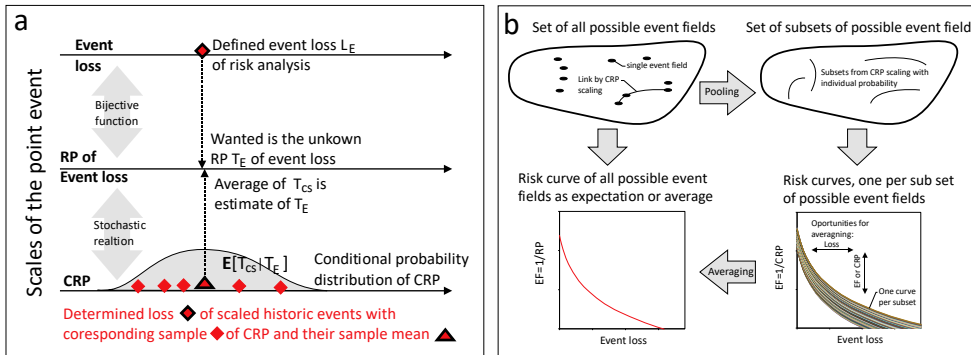
The estimation is based on following stochastic relations and assumptions (or proxies)

$$T_E(L_E) = E[T_{CS}(L_E)], L_E(T_E) = E[L_E(T_{CS} = T_E)], \text{ and } \Lambda_E(L_E) = E[1/T_{CS}(L_E)], \quad (16)$$

The origin is (5); the well-known delta method (Coles, 2011) for computation of propagation of errors is also a base. A more
 300 illustrative explanation is provided for the loss scaling by Figure 6 a. The sample mean (sample average) of corresponding
 CRPs is the estimate for their expectation and thereby the estimate of RP of event loss. Figure 6 b offers a further stochastic
 interpretation. The basic set includes all possible events which match with the risk curve. In addition, every possible wind field
 has a CRP. This also provides a link between some of the possible event fields – the CRP scaling and pools wind fields to
 subsets. The actual probability density of an observation of a random variable is mostly not known. In the same way, each
 305 “observed” subset has an unknown probability (density). And each subset corresponds to a risk curve. Their expectation
 determines the risk curve of the entire set of event fields and is estimated by the average of a sample of linked event fields



since the expectation of a random variable is estimated by the corresponding sample mean. Three averaging variants are possible.



310 **Figure 6: Schemes of the scaling-averaging approach: a) Averaging of CRP in relation to the different scales of NatCat as point event, and b) set of possible event fields as set of subsets with corresponding risk curves.**

5 Conclusion, discussion, and outlook

5.1 General

CRP opportunities prove once again that mathematical statistics and stochastic is the central technology for analysis, modeling, and understanding risks such as NatCat. The CRP is a simple, reasonable, and testable stochastic measure for a catastrophe. In addition, the new approach offers the scaling of historical event fields under stochastic control. By this and a simple exposure and vulnerability model, the risk curve for insured winter storm losses in Germany could be derived. Our risk curves for Germany have a similar course as these by vendors (Figure 3 d). The risk assumption by EU for Germany with RP 200 years is significantly higher than ours. The estimate by Donat et al. (2011) differs significantly and seems to be implausible. A reason might be their statistical modeling by the generalized Pareto distribution as already applied for wind losses by Pfeifer (2011). The tapered Pareto distribution (Schoenberg and Patel, 2012) or a similar approach (Raschke, 2020) is a more appropriate proxy for our risk curve's tail.

The advantage of our approach over classical vendor models for winter storm risk is the simplicity and clarity about the assumptions. Probabilistic vendor models need tens of thousands of simulated storms (Mitchell-Wallace et al. 2017) with unpublished or even unknown (implicit) assumptions on hazard and loss estimates for a defined RP. We have only scaled 16 event fields of historical storms with controlled stochastic (probabilistic) and could even quantify the SE. The three variants of averaging result in remarkably similar outcomes.

A reasonable weighting for the CRP might depend on the examined peril. The expected annual sum of local losses might be a universal weighting since the sum of local expectations determines the expectation of total annual loss. The various weighting opportunities also underline the fact that there is not an absolute view on hazard and risk.



5.2 Requirements of the new approach

Our approach to CRP is based on two assumptions. At first, the local and global events occur as a Poisson process. This is frequently used in extreme value statistics (Coles, 2001) and can be statistically tested (Stephens, 1986). Moreover, the detected clustering (overdispersion) of winter storms over Germany (Karremann et al., 2014) is statistically not relevant for higher RP
335 (Raschke, 2015). With increasing RP, the number of occurring winter storms converges to a Poisson distribution. Clustering is also influenced by the event definition, which is not the topic here (catchword declustering; Coles, 2001). We also point out that the assumed Poisson process needs not be homogenous during the defined unit period (year, season, or half-season).

The second prerequisite is robust knowledge about the local RP by a local hazard curve. As it is described in *Section 3*, the statistical estimation is not trivial since bias correction can be required. The distinction between different perils, such as
340 thunderstorms and winter storms, maybe an issue. Furthermore, there are no appropriate models for the local hazard every peril and region; for example, hail in Europe, we only know local hazard curves for Switzerland by Stucki et al., (2007) and these were roughly estimated.

5.3 The spatial dependence

Our loss estimates for higher RP depend on the assumption for spatial dependency – with or without max-stability. In
345 consequence, questions arise for all NatCat models, which are based on generated event fields. Is the spatial dependence max-stable or not? Is the (implicit) dependence model sufficient? How is this validated? As far as we know, these are not well considered in previous models. The issue is only a marginal note in the book by Mitchell-Wallace et al. (2017) Raschke's et al. (2011) winter storm model for Switzerland implies max-stability without a validation. Jongman's et al. (2014) model for European floods considers dependence explicitly. However, their assumptions and statistical inference are not appropriate
350 according to Raschke (2015). In statistical journals, max-stable dependence models have been applied to natural hazards without a systematic test of the dependence assumption, such as the snow model by Blanchet and Davison (2011) for Switzerland and the river flood model by Asadi et al. (2015) for the Upper Danube river system. The models for European winter storms (extratropical cyclones), that base on numerical simulations (Della-Marta et al., 2010; Schwierz et al., 2010; Osinski et al., 2016), are subject to the same weakness; spatial dependence is not intensively validated.

In the copula-based research by Bonazi et al. (2012) and Dawkins and Stephenson (2018), the local extremes of European
355 winter storms are sampled by a pre-defined list of significant events. Such sampling is not foreseen in extreme value statistics (Coles, 2010). Block maxima and (declustered) POT are the established sampling methods. We have analyzed the dependence between block maxima, which are random variables. It is also possible to analyze stochastic associations between de-clustered peak over thresholds (POT, local point events), as Asadi et al. (2015). Further arguments against the extreme value sampling
360 by a pre-defied event list: It is not ensured that all local extremes of the peril are considered since the storm list is not complete (smaller events are missed). In addition, European winter storm frequently does not cover Europe entirely. By this, paired observations are not ensured even though this is needed for the bivariate copula approach.



However, the copula approach for the dependence of random variables (Marie and Kotz, 2001) is a bit similar to our research of associated local point events. In both cases, the physical quantities of the margins are replaced by uniform quantities –
365 uniformly distributed random variables or RPs.

5.4 Opportunities for future research

Since the current model for the local hazard of winter storms over Germany results in considerable uncertainty, it should be improved in the future. This could be realized by a kind of regionalization as already known in flood research (Merz and Blöschl, 2003; Hailegeorgis and Alfredsen, 2017). Besides, more wind stations could be considered in the analysis with better
370 consideration of incompleteness in the records. An extension of the observation period is conceivable if homogeneity of records and sampling is ensured. A more sophisticated approach might be used to discriminate the local extremes of winter storms from other windstorm perils. The POT methods (Coles, 2001; Beirlant et al., 2004) could then be used in the analysis.

The vulnerability model results in the largest share of the uncertainty of our risk estimate even though the loss function's determined parameters imply further uncertainty. More and more detailed loss data can only improve this issue. Nevertheless,
375 our loss function is reasonable according to previous models for Germany (Figure 6b). The influence of deductibles (Munich Re, 2002) per insured object is not explicitly considered but smoothed in our approach.

Further opportunities for improvements in the winter storm modeling are conceivable. The event field might be more detailed reproduced/interpolated as done by Jung and Schindler (2019). They have considered the roughness of land cover at a regional scale besides further attributes. However, they did not consider the local roughness of immediate surroundings as discussed
380 by Wichura (2009) by the example of wind station Potsdam (Germany). He assumes that decreasing wind hazard for around 100 years is (also) a result of the development of vegetation and land use in contrast to the interpretation by Mudelsee (2020). However, our sampling period of 20 years should not be influenced so much by long-term changes.

We also see research opportunities for the community of mathematical statistics, especially extreme value statistics. The link between normalized area functions, CV, and relation dependence to distance is of great interest. Our construction for the non-
385 max stable scaling is just a workaround to illustrate the consequences of dependence characteristics. Transparent stochastic models are needed. Estimation methods could also be extended and examined, such as the bias in estimates of RP. This bias might imply consequences for the broader research community.

6 Code and data availability

A special code was not generated or used. Our computations had been simply carried out by MS Excel. The wind data were
390 downloaded from server of German meteorological service (Deutscher Wetter Dienst, 2020). The exposure data were provided by UNISDR (2015). The loss data are part of the downloaded report of General Association of German Insurer (Gesamtverband Deutscher Versicherer, 2019). The here considered wind stations and storms are listed in Supplementary (Excel file).



7 Author's contribution

The author has derived the theory, carried out analysis and wrote the paper. External help has been used regarding proofreading.

395 8 Competing interest

The author declare that he has no conflict of interest.

9 Acknowledgement

The author thanks the proofreaders.

References

- 400 Asadi P., Engelke S. and Davison A.C. Extremes on river networks. *Ann. Appl. Stat.* **9**, 2023-2050, 2015.
Beirlant, J., Goegebeur, Y., Teugels, J. and Segers, J. *Statistics of Extremes – Theory and Application*. Book Series: Wiley
Series in Probability and Statistics, John Wiley & Sons, 2004.
Blanchet, J. & Davison A.C. Spatial Modelling of extreme snow depth. *The Annals of Applied Statistics* **5**, 1699-1725,
2011.
- 405 Bonazzi, A., Cusack, S., Mitas, C. and Jewson, S. The spatial structure of European wind storms as characterized by
bivariate extreme-value Copulas. *Nat. Hazards Earth Syst. Sci.* **12**, 1769-1782, 2012.
Bormann, P. and Saul, J. Earthquake Magnitude, in *Encyclopedia of Complexity and Applied Systems Science*, 3, pp.
2473-2496, <http://gfzpublic.gfz-potsdam.de/pubman/item/escidoc:238827:1/component/escidoc:238826/13221.pdf>,
2009.
- 410 Coles, S. *An Introduction to Statistical Modeling of Extreme Values*. Book Series: Springer Series in Statistics, Springer,
2001.
Conover, W.J. *Practical Nonparametric Statistics*. New York: John Wiley & Sons. Pages 309–314, 1971.
Cook, N.J. *The Designer's Guide to Wind Loading of Building Structures. Part 1: Background, Damage Survey, Wind
Data and Structural Classification*. Building Research Establishment, Garston, and Butterworths, London, pp371,1986.
- 415 Dawkins, L.C. and Stephenson, D.B. Quantification of extremal dependence in spatial natural hazard footprints:
independence of windstorm gust speeds and its impact on aggregate losses. *Nat. Hazards Earth Syst. Sci.* **18**, 2933-2949,
2018.
De Haan, L. A spectral representation for max-stable processes. *The Annals of Probability* **12**, 1194-1204, 1984.
Della-Marta, P., Mathias, H., Frei, C., Liniger, M., Kleinn, J. & Appenzeller, C. The return period of wind storms over
420 Europe. *International Journal of Climatology* **29**, 437-459, 2009.
Della-Marta, P.M., Liniger, M. A., Appenzeller, C., Bresch, D. N, Koellner-Heck, P. and Muccione, V. Improved estimates
of the European winter windstorm climate and the risk of reinsurance loss using climate model data. *Journal of Applied
Meteorology and Climatology* **49**, 2092-2120, 2010.
Deutsche Rück, *Sturmdokumentation*, www.deutscherueck.de/downloads/sturmdokumentation/, (download 2020)
425 Deutscher Wetter Dienst (DWD, German meteorological service), Climate Data Centre (CDC),
<https://cdc.dwd.de/portal/202007291339/index.html> (download Spring 2020).
Donat, M. G., Pardowitz, T., Leckebusch, G. C., Ulbrich, U. and Burghoff, O. High-resolution refinement of a storm loss
model and estimation of return periods of loss-intensive storms over Germany. *Nat. Hazards Earth Syst. Sci.* **11**,
2821-2833, 2011.



- 430 European Commission. Valuation and risk-based capital requirements (pillar i), enhanced governance (pillar ii) and
increased transparency (pillar iii), COMMISSION DELEGATED REGULATION (EU) 2015/35 supplementing
Directive 2009/138/EC of the European Parliament and of the Council on the taking-up and pursuit of the business of
Insurance and Reinsurance (Solvency II), 2014.
- 435 European Union (EU). Eurocode 1: Actions on structures – Part 1-4: General actions – Wind actions. The European Union
per Regulation 305/2011, Directive 98/34/EC, Directive 2004/18/EC, 2005.
- Falk, M., Hüsler, J., and Reiss, R.-D. *Laws of Small Numbers: Extremes and rare Events*. Birkhäuser 3rd ed., Basel, 2011.
Gesamtverband Deutscher Versicherer (GDV, General Association of German Insurer), *Naturgefahrenreport - Serviceteil*
(German, www.gdv.de/de/zahlen-und-fakten/publikationen/naturgefahrenreport), 2019.
- 440 Guse, B., Merz, B., Wietzke, L., Ullrich, S., Viglione, A. and Vorogushyn, S. The role of flood wave superposition in the
severity of large floods. *Hydrol. Earth Syst. Sci.* **24**, 1633-1648, 2020.
- Harris, R. I. Gumbel re-visited – a new look at extreme value statistics applied to wind speeds. *J. Wind Eng. Ind. Aerodyn.*
59, 1-22, 1996.
- Hailegeorgis, T.T. and Alfredsen, K. Regional flood frequency analysis and prediction in ungauged basins including
estimation of major uncertainties for mid-Norway. *Journal of Hydrology: Regional Studies* **9**, 104-126, 2017.
- 445 Heneka, P. and Ruck, B. A damage model for assessment of storm damage buildings. *Engineering Structures* **30**, 721-733,
2008.
- Jongman, B., et al. Increasing stress on disaster-risk finance due to large floods. *Nature Clim. Change* **5**, 264-268, 2014.
- Jung, C. and Schindler, D. Historical Winter Storm Atlas for Germany (GeWiSA). *Atmosphere* **10**, 387, 2019.
- Karremann M.K., Pinto J.G., von Bomhard P.J. and Klawa M. On the clustering of winter storm loss events over Germany,
Nat Hazards Earth Sys **14**, 2041-2052, 2014.
- 450 Klawa, M. & Ulbrich, U. A model for the estimation of storm losses and the identification of severe winter storms in
Germany. *Nat. Hazards Earth Syst. Sci.* **3**, 725-732, 2003.
- Landwehr, M.J., Matalas, N. C. & Wallis, J. R. Probability weighted moments compared with some traditional techniques
in estimating Gumbel Parameters and quantiles. *Water Resources Research* **15**, 1055-1064, 1979.
- 455 Lindsey, J. K. *Parametric statistical inference* Clarendon Press, Oxford, 1996.
- Mari, D. and Kotz, S. *Correlation and Dependence*. Imperial College Press, 2001.
- Merz, R. and Blöschl, G. A process typology of regional floods. *Water Resources Research* **19**,
doi.org/10.1029/2002WR001952, 2003.
- Mitchell-Wallace, K., Jones, M., Hiller, J., and Foote, M. *Natural catastrophe Risk Management and Modelling -*
Practitioner's Guid. Wiley Blackwell, Chichester, UK, 2017.
- 460 Mudelsee, M. Statistical analysis of climate extremes. Cambridge University Press, Cambridge, pp 124-129, 2020.
- Munich RE GeoRisks Research Department Winter Storms in Europe (II) Analysis of 1999 losses and loss potentials,
2002.
- National Hurricane Centre, Saffir-Simpson Hurricane Wind Scale, web page www.nhc.noaa.gov/aboutsshws.php (last
download Spring 2020).
- 465 Osinski, R. et al. An approach to build an event set of European windstorms based on ECMWF EPS. *Nat. Hazards Earth*
Syst. Sci. **16**, 255-268, 2016.
- Pfeifer, D. Study 4: Extreme value theory in actuarial consulting: windstorm losses in Central Europa. In: R.-D. Reiss &
M. Thomas: *Statistical Analysis of Extreme Values – with Applications to insurance, finance, hydrology and other*
470 *fields*. 2nd Ed., Birkhäuser, Basel, 373-378, 2011.
- Raschke, M., Bilis, V. and Kröger, W. Vulnerability of the Swiss electric power grid against natural hazards. In
Proceedings of 11th International Conference on Applications of Statistics and Probability in Civil Engineering
(ICASP11), Zurich, Switzerland, 2011.
- 475 Raschke, M. Statistical modelling of ground motion relations for seismic hazard analysis. *Journal of Seismology* **17**,
1157-1182, 2013.
- Raschke, M. Statistical detection and modeling of the over-dispersion of winter storm occurrence. *Nat. Hazards Earth Syst.*
Sci. **15**, 1757-1761, 2015.
- Raschke, M. Statistics of flood risk. *Nature Clim. Change* **4**, 843-844, 2015.



- 480 Raschke, M. Alternative modelling and inference methods for claim size distributions. *Annals of Actuarial Science* **14**, 1-19, 2020.
- Roberts, J. et al. The XWS open access catalogue of extreme European windstorms from 1919 to 2012. *Nat Haz Earth Sys Sci* **14**, 2487-2501, 2014.
- Schlather, M. Models for Stationary Max-Stable Random Fields. *Extremes* **5**, 33–44, 2002.
- 485 Schwierz, C., Köllner-Heck, P., Zenklusen Mutter, E. et al. Modelling European winter wind storm losses in current and future climate. *Climatic Change* 101, 485–514, 2010.
- Schoenberg, F.P. and Patel, R.D. Comparison of Pareto and tapered Pareto distributions for environmental phenomena. *Eur. Phys. J. Spec. Top.* **205**, 159–166, 2012.
- Statistisches Bundesamt (German Office statistics) Preisindizes für die Bauwirtschaft – Mai 2020 (2020).
- 490 Stephens M.A. Test based on EDF statistics. in D’Augustino, RB, Stephens, MA (Editors) *Goodness-of-Fit Techniques. statistics: textbooks and monographs*, Vol. 68, Marcel Dekker, New York, 1986.
- Stucki, M., & Egli, T. *Synthesebericht - Elementarschutzregister Hagel*. Präventionsstiftung der Kantonale Gebäudeversicherungen, ISBN 978-3-9523300-0-5, 2007.
- UNISDR, Global Assessment Report (GAR)Global exposure dataset - population and environmental built, <https://data.humdata.org/dataset/exposed-economic-stock>, last down load 2020, 2015.
- 495 Upton, G. and Cook, I. *A dictionary of statistics*. 2nd rev. Ed., Oxford University Press, 2008.
- Waisman, F. European windstorm vendor model comparison (and panel discussion). In *Slides of a presentation at IUA catastrophe risk management conference*, London **30**, (https://www.iua.co.uk/IUA_Member/Events/Catastrophe_Risk_Management_Presentations/European_Windstorm_Vendor_Model_Comparison.aspx) 2015.
- 500 Wichura, B. Analyse standortbezogener Windklimatologien als Eingangsgröße für die Bemessung von Bauwerken nach der DIN 1055-4. In book: *Windingenieurwesen in Forschung und Praxis* (pp.157-168) Edition: *WiG-Berichte* **11**, Windtechnologische Gesellschaft e.V., Editor: Udo Peil, 2009.